Desalination and Water Treatment
www.deswater.com
doi: 10.1080/19443994.2015.1111807

57 (2016) 20661–20670
September

Taylor & Francis
Taylor & Francis Group

Application of nanofiltration pretreatment to remove divalent ions for economical seawater reverse osmosis desalination

Minho Park[a], Jongkwan Park[b], Eunkyung Lee[c], Jeehyeong Khim[d], Jaeweon Cho[b,*]

[a]*Plant & Environment Research Team, Daewoo E&C, Suwon, Korea, Tel. +82 31 250 1206; Fax: +82 31 250 1130; email: minho.park@daewooenc.com*
[b]*School of Urban and Environmental Engineering, Ulsan National Institute of Science and Technology (UNIST), 50 UNIST-gil, Ulju-gun, Ulsan 689-798, Korea, Tel. +82 52 217 2833; Fax: +82 52 217 2819; email: jaeweoncho@unist.ac.kr (J. Cho)*
[c]*Water Resource Research Team, KCC Central Research Institute, 17-3 Mabuk-ro 240beon-gil, Giheung-gu, Yongin-si, Gyeonggi-do, Korea, Tel. +82 31 288 3037; Fax: +82 31 288 3015; email: eklee@kccworld.co.kr*
[d]*School of Civil, Environmental and Architectural Engineering, Korea University, Seoul, Korea, Tel. +82 2 3290 3318; Fax: +82 2 928 7656; email: hyeong@korea.ac.kr*

Received 2 September 2014; Accepted 18 October 2015

ABSTRACT

To minimize scale formation potential in the applications of reverse osmosis (RO) membranes as a pretreatment unit, relatively loose nanofiltration (NF) membrane systems coupled with ultrafiltration (UF) were used to remove divalent ions from seawater. However, the UF did not reject any ions because of pore size. The rejection of divalent ions by NF was in order of sulfate (>95%), magnesium (>60%), and calcium (>30%) in every rejection experiment based on water recovery rate (40, 50, 60, 70, and 80%). In the UF/NF/RO hybrid pilot system, most of the divalent (>99%) and the monovalent (>97%) ions were effectively rejected with slightly increased divalent ion rejection compared to the UF/RO system. Seawater temperature influenced rejection of ions with regards to either the diffusion- or convection-dominant transport of ions through the membrane pores. Electric power consumption was also compared between the UF/NF/RO process and the UF/RO process. For different salinity conditions (28,000 and 45,000 mg/L of total dissolved solids), the lowest energy consumption by NF/RO was 3.3 and 6 kWh/m^3 with recovery of 80% for NF and 40% for RO, respectively.

Keywords: Desalination; Nanofiltration; SWRO; Divalent ions; Scaling; Energy consumption

1. Introduction

Over the last few decades, desalination has been recommended as a possible solution to the water shortage problem worldwide [1]. Among various desalination processes, reverse osmosis (RO) membrane processes have achieved high efficiencies (>99%) in removing salts to produce fresh water from seawater [1,2]. According to the 24th International Desalination Association (IDA) Worldwide Desalting Plant Inventory (2012) [3], 747 new plants were established in 2011. The report estimated the global desalination capacity to be 77.4 million m^3/d (20,449 MGD) with 15,988 plants; this market growth was due to development of advanced seawater RO (SWRO)

*Corresponding author.

desalination techniques with improved energy efficiency. However, SWRO desalination still has limitations, such as fouling, scaling, high-energy cost, and limited water recovery [4,5]. Among those, scaling has been one of the significant problems in SWRO desalination process. Due to high salt rejection of SWRO, the inorganic compounds are concentrated and precipitate on the membrane surface, which leads to scaling. This can cause flux decline, which increases the energy consumption and maintenance costs especially in RO system [1,2,6]. To overcome the scaling problem, many research groups have applied various pretreatments to remove salts prior to RO process; acidity (i.e. pH) adjustment, addition of antiscalants, and nanofiltration (NF) membrane treatment [7,8]. Among various pretreatment options, NF is effective in preferentially rejecting divalent ions from seawater [7,9,10]. Peter Eriksson et al. reported that NF membrane rejected sulfate ions with rejection efficiency higher than 99% and other divalent cations at 80–95% [9]. Another study has investigated the rejection of compounds leading to scaling by commercially available NF membranes, where 60% rejection of bicarbonate, an important ion to produce $CaCO_3$ scalant, was presented, and 60–70% of rejection of various other divalent ions by NF was reported [11].

Energy consumption is another considerable factor in SWRO desalination. Although SWRO desalination is more economical than thermal desalination, energy consumption in SWRO process needs to be further reduced since it is related to total water production cost. The energy consumed by various SWRO systems investigated are in the range 3.7–5.3 kWh/m^3 [12–14]. According to Drioli et al. NF followed by SWRO system showed energy consumption of 4.5 kWh/m^3 [15] and 3.7 kWh/m^3 [16] in two different studies. The estimated energy consumption may vary depending on RO or NF/SWRO desalination system capacities, but it is important to optimize energy consumption for desalination designed for various purposes.

Both salt concentration and temperature of seawater are important parameters influencing the efficacies of NF/SWRO desalination processes. For example, as seawater temperature increases, salt rejection by NF membranes decreases (i.e. from diffusion dominant process), and water permeation increases according to the Arrhenius relation [17]. Different seawater temperatures and the percentage salt rejection have been monitored for NF/SWRO processes to evaluate the effect of seawater temperature on desalination performance using membrane.

In this study, to determine optimal operation conditions for NF/SWRO desalination, the salt rejection efficiencies of NF membranes as a pretreatment system for SWRO membranes were investigated under various recovery conditions. The effect of feed water temperature on NF membrane performance was demonstrated, and energy consumptions were monitored with two different membrane desalination systems (either NF/SWRO or SWRO).

2. Materials and methods

2.1. Sampling site and pilot system description

The pilot plant system used for this study was located near the city of Incheon, Korea. The feed seawater, obtained from the Yellow Sea, was purchased from a seawater distributor. The seawater was filtered by the distributor using sand filtration. Characteristics of the feed water are listed in Table 1. The temperature and the total dissolved solid (TDS) concentration of the seawater used in ultrafiltration (UF) feed water were measured on-site; these values exhibited seasonal fluctuations, from 3.6℃ and 31,000 mg/L in winter to 28.5℃ and 28,000 mg/L in summer.

The pilot plant system consisted of UF/NF/RO modules in series to compare the performances of UF/NF, UF/RO, and UF/NF/RO systems, with respect to water qualities and energy effectiveness. A schematic of the UF/NF/RO hybrid pilot plant is illustrated in Fig. 1

Table 1
Feed water characteristics

	Concentration (mg/L)			Concentration (mg/L)	
Anions	Seawater	Designed seawater[a]	Cations	Seawater	Designed seawater[a]
Chloride	17,000 ± 2,500	27,000 ± 1,600	Sodium	9,700 ± 390	16,000 ± 1,000
Sulfate	2,300 ± 140	2,400 ± 140	Magnesium	1,100 ± 46	2,000 ± 140
Bromide	44 ± 6.2	63 ± 14	Calcium	330 ± 17	620 ± 70
Fluoride	0.90 ± 0.04	6.3 ± 8.4	Potassium	310 ± 17	580 ± 36

[a]Reuse of RO concentrate as feed water for simulating Middle East sea (TDS = 45,000 mg/L).

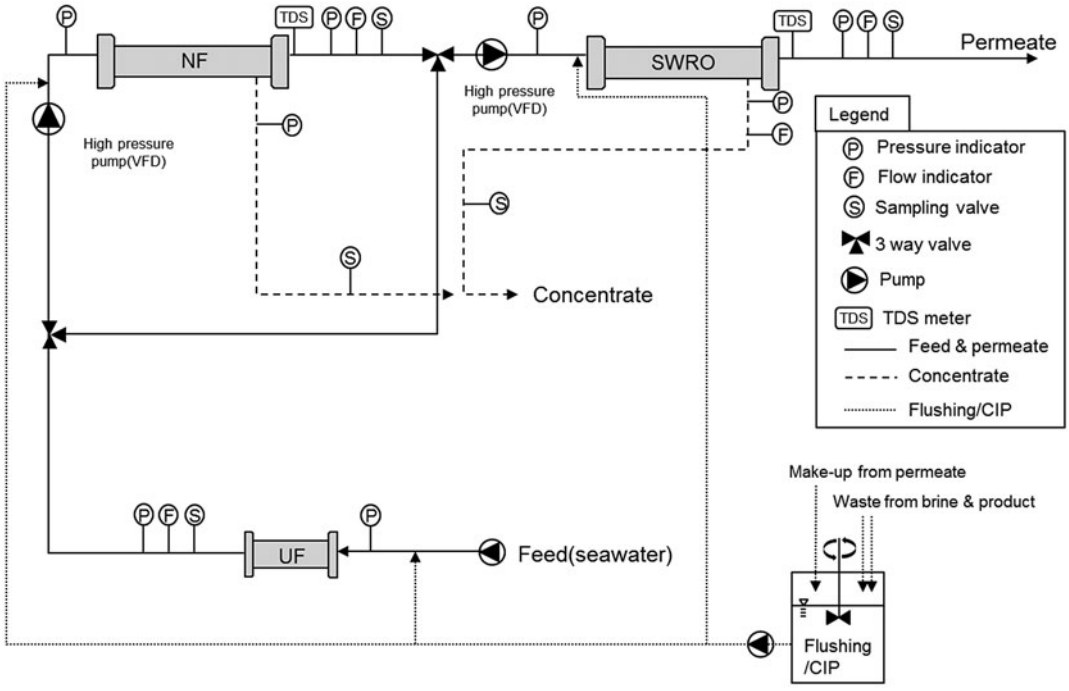

Fig. 1. Schematic flow diagram of NF/RO hybrid pilot plant. Feed water was filtrated through UF process to evaluate the exclusive effect of salts on NF, RO, and NF-RO process.

Table 2
Description of selected membranes provided by manufacturer and other previous researches

	UF	NF	RO
Membrane model	GUF-6050ES	NF270-4040	SW30-4040
Manufacturer	Pure Envitech	Dow Filmtec	Dow Filmtec
Membrane type	Polysulfone	Polyamide thin-film composite	Polyamide thin-film composite
MWCO (Da)/Pore size	100 K/0.1 μm[a]	300 [21]/0.84 nm [22]	Not available
Pure water permeability ($L\ m^{-2}\ h^{-1}\ bar^{-1}$)	204.1[b]	14.0 [22]	1.23 [22]
Salt rejection (%)	–	40–60[c], >97[d]	99.4[e]
Zeta potential at pH 7 (mV)	–	−32.6 [23] approx. −24 [22]	approx. −14 [22]
Root mean square roughness (nm)	–	9.0 (±4.2) [23]	approx. 71 [24]
Contact angle (°)	–	28 (±2) [22]	62.0 (±7.2) [22]

[a]Provided by manufacturer.
[b]Provided by manufacturer (0.98 bar pressure).
[c]Tested condition by manufacturer (500 mg/L $CaCl_2$, 5 bar pressure).
[d]Tested condition by manufacturer (2,000 mg/L $MgSO_4$, 5 bar pressure, recovery 15%).
[e]Tested condition by manufacturer (32,000 mg/L NaCl, 55 bar pressure, recovery 4–10%).

and a detailed description of membrane modules used in each system is summarized in Table 2. The UF membrane modules were equipped with polysulfone hollow-fiber UF membranes (GUF-6050ES, Pure Envitech Co., Ltd, Korea). Six modules of 4-inch polyamide-based thin-film composite (TFC) NF membranes (NF270-4040, Dow Filmtec, Midland, MI) in one pressure vessel were used as the NF unit to remove divalent ions prior to SWRO. Permeate of the NF unit was used as feed water for a 4-inch polyamide-based

Table 3
Operational conditions for evaluating NF, RO, and NF/RO perfomance

Feed water	Process (Membrane)	Q_f[a] (m^3/d)	TDS_f[b](mg/L)	Recovery (%)		
				NF (flux: lmh)	RO (flux: lmh)	System
Seawater	NF270	40	28,000	40–80 (13–26)	–	40–80
	NF270-SW30	40	28,000	80 (26)	12.5–62.5 (5–25)	10–50
	SW30	40	28,000	–	10–50 (4–20)	10–50
Designed seawater	NF270	40	45,000	40–80 (13–26)	–	40–80
	NF270-SW30	40	45,000	80 (26)	12.5–50 (5–20)	10–40
	SW30	40	45,000	–	10–40 (4–16)	10–40

[a]Q_f indicates flow rate of feed water.
[b]TDS_f indicates TDS of feed water.

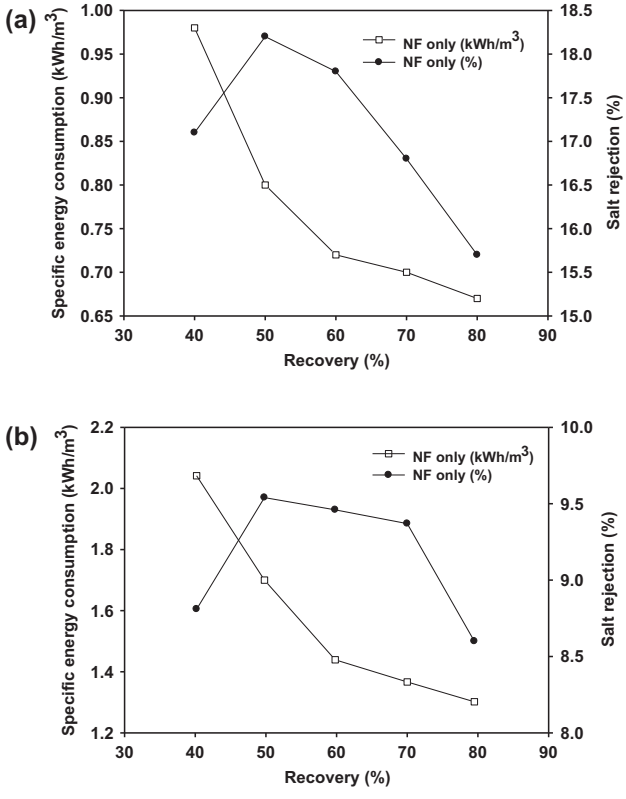

Fig. 2. Specific energy consumption and salt rejection (%) of NF only system for (a) raw seawater and (b) designed seawater samples with various recovery ratio.

TFC RO membrane (SW30-4040, Dow Filmtec, Midland, MI) unit (6 modules in one vessel).

A high-pressure displacement pump (APP 1.8, Danfoss™, Denmark) was placed in front the NF and RO units. Flow rate was controlled by a variable frequency device (VFD) (Model iG5A, LSIS Co., Ltd, Korea) to feed a predesignated flow rate. As shown in Fig. 1, electric devices were equipped and calibrated to measure the operational parameters, such as pressure (Model KP-200, Corea Flow Co., Ltd, Korea), flow rate (Type 2536 Rotor-X, Georg Fischer Ltd, Switzerland), temperature (KT-10, Corea Flow Co., Ltd, Korea), and electrical power consumption (LGRW34-2210, LSIS Co., Ltd, Korea); all the data obtained were stored in a data acquisition system. The UF, NF, and RO units were automatically operated using a programmable logic controller (PLC) under the designed experimental conditions. Conventional cleaning-in-place (CIP) was applied to offset the effects of previous.

2.2. Pilot plant operation

The UF/NF, UF/NF/RO, and UF/RO experiments were conducted at varying recovery ratios to evaluate salt rejection and energy consumption, as tabulated in Table 3. Operation time and feed flow rate for each experiment was 150 min and 40 m^3/d, respectively. Two different seawater samples were applied as feed water to NF and RO membranes. One was seawater from the Yellow Sea, and the other was a designed seawater to simulate Middle East seawaters, so as to investigate the applicability of the NF/RO system

Table 4
Permeate water quality of UF-NF, UF-RO, and UF-NF-RO

Recovery (%)	Concentration (mg/L)						
	Chloride	Sulfate	Sodium	Magnesium	Calcium	Potassium	TDS
UF-NF							
40	23,600 (±700)	130 (±30)	15,100 (±400)	770 (±60)	400 (±2)	550 (±10)	24,470 (±70)
50	22,000 (±1,800)	190 (±20)	14,100 (±1,100)	630 (±60)	390 (±3)	540 (±9)	24,080 (±50)
60	22,600 (±1,600)	166 (±50)	14,500 (±900)	660 (±40)	360 (±6)	530 (±3)	24,140 (±60)
70	22,700 (±1,100)	180 (±40)	15,700 (±200)	710 (±40)	380 (±2)	550 (±9)	23,220 (±80)
80	23,100 (±1,900)	120 (±20)	15,300 (±300)	730 (±50)	370 (±10)	550 (±30)	22,630 (±60)
UF-RO							
10	520 (±20)	27 (±1)	540 (±6)	7 (±0)	2 (±0)	22 (±0)	1,177 (±30)
20	440 (±2)	16 (±1)	420 (±5)	4 (±0)	1 (±0)	16 (±0)	931 (±0)
30	350 (±10)	11 (±1)	330 (±10)	3 (±0)	1 (±0)	13 (±0)	704 (±0)
40	350 (±5)	9 (±0)	310 (±4)	3 (±0)	1 (±0)	12 (±0)	647 (±0)
UF-NF-RO							
10	920 (±40)	1 (±0.5)	720 (±10)	2 (±0)	1.4 (±0)	23 (±1)	154 (±0)
20	640 (±10)	0.5 (±0)	520 (±10)	1.3 (±0)	0.9 (±0)	16 (±1)	102 (±0)
30	540 (±50)	0.3 (±0)	440 (±4)	1.1 (±0)	0.8 (±0)	13 (±1)	102 (±0)
40	590 (±50)	0.3 (±0)	400 (±21)	1 (±0)	0.8 (±0)	12 (±1)	102 (±0)

under relatively higher salinity. All the feed seawater was filtered using UF membranes and fed to NF and RO membranes. For the production of designed seawater, RO concentrate was prepared with TDS of 45,000 mg/L, at ~40% recovery, and 6 m^3 of RO concentrate was used for each set of experiment. Feed, permeate, and concentrate were collected thrice from each experiment through sampling valves and were analyzed in terms of salt concentration (mg/L) to observe the salt rejection. Specific energy consumption (kWh/m^3) was calculated at 25˚C to estimate economic feasibility through measurements of both energy consumption and permeate volume during operation. For comparison, the energy consumption was measured both before and after the operation, by an electric meter (LGRW34-2210, LSIS Co., Ltd, Korea). Changes in pressure, flow rate, and temperature were monitored to demonstrate the effects of the operating conditions on membranes performance of UF, NF, and RO systems. Feed flow rate and recovery of the UF unit were set at 45 m^3/h and 95% (flux = 59 lmh) to maintain a constant feed flow rate to the NF and RO units. Feed flow rate was determined considering membrane cleaning time and recovery ratio. The initial transmembrane pressure (TMP) was 0.4 bar. Each operation cycle was 30 min long (filtration for 28 min, back washing for 1 min, and flushing for 1 min).

NF experiments were performed with different recovery ratios from 40% (flux = 13 lmh) to 80% (flux = 26 lmh) and evaluated in terms of salt rejection (including divalent ions) and energy consumption, to find the optimum condition for NF operation. To compare the NF/RO combination with RO, the end salt rejections and specific energy consumptions were assessed with identical overall recovery ratios varying from 10% (flux = 4 lmh) to 50% (flux = 20 lmh). Recovery ratio of NF in the NF/RO operation was set

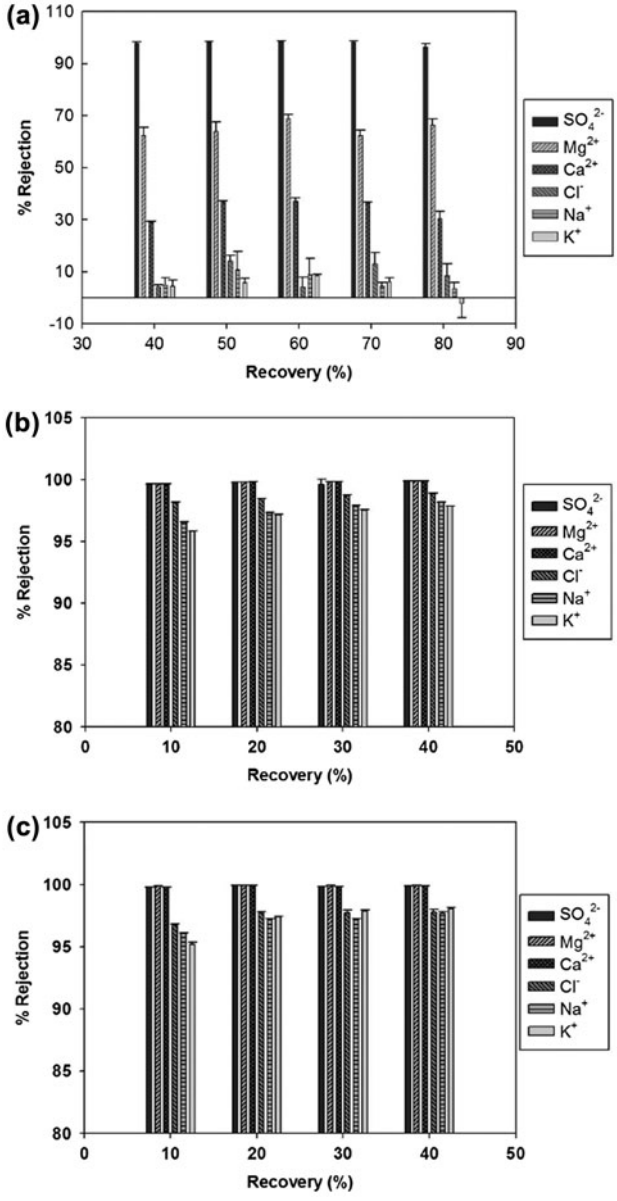

Fig. 3. Monovalent and divalent ion rejection (%) as function of different recoveries, during the (a) UF/NF, (b) UF/RO, and (c) UF/NF/RO operations.

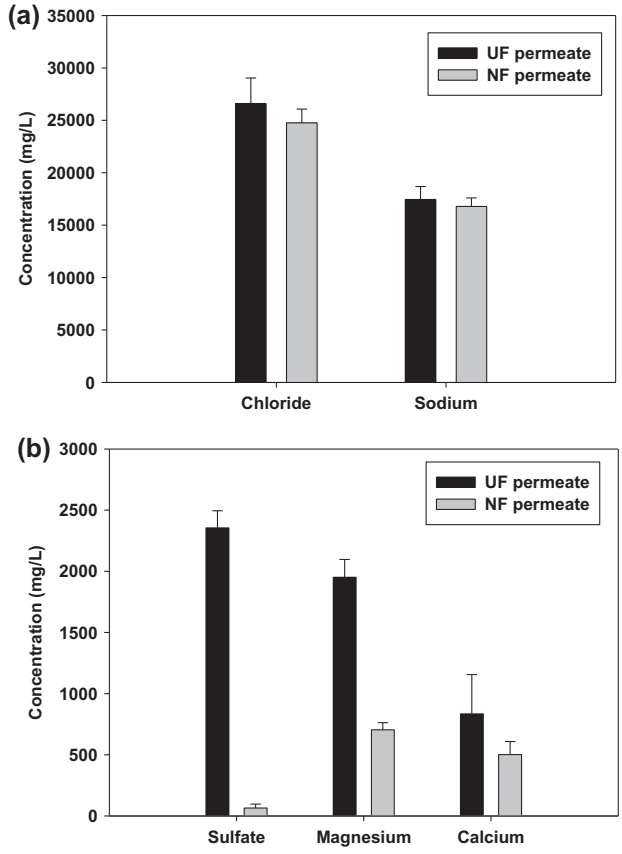

Fig. 4. Concentration of (a) monovalent ions and (b) divalent ions in UF permeate (NF feed water) and UF/NF permeate (SWRO feed water).

to 80%, which gives the lowest specific energy consumption compared to other recovery ratios (Fig. 2). As the NF permeate was fed to the RO unit in the NF/RO process, the characteristics of the NF permeate directly influence RO performance. The effect of temperature on NF performance was intermittently monitored for each set of operations. Seasonal experiments were conducted, from winter to summer, with both seawater and the designed seawater. CIP was conducted when TMP of the UF membrane reached 1.5 bar, then, TMP was restored to the initial value of 0.4 bar. The chemicals used for cleaning the UF were 0.1 M citric acid and 0.5% sodium chlorite, and 0.2% hydrochloric acid, 1.0% sodium hydrosulfite, and 0.1% sodium hydroxide were used for cleaning of NF and RO. No changes in the normalized performance data of NF and RO were detected after CIP was applied on the UF system, followed by the NF and RO systems, indicating that NF and RO were not fouled by organic matters or scalants. During operation, there were no significant TMP increase and flux decline in the NF and RO systems; hence, no antiscalant was added in this study and no study on the comparison of scale formation was carried out.

2.3. Water quality characterization

Temperature, conductivity, and TDS were all measured *in situ*. Other water quality characteristics were also analyzed after prefiltration using 0.7 μm glass macrofiber filters (GFF, Whatman, Maidsone, England). Ions were analyzed using ion chromatography: ICS-90 (Dionex, Sunnyvale, CA, USA) equipped with

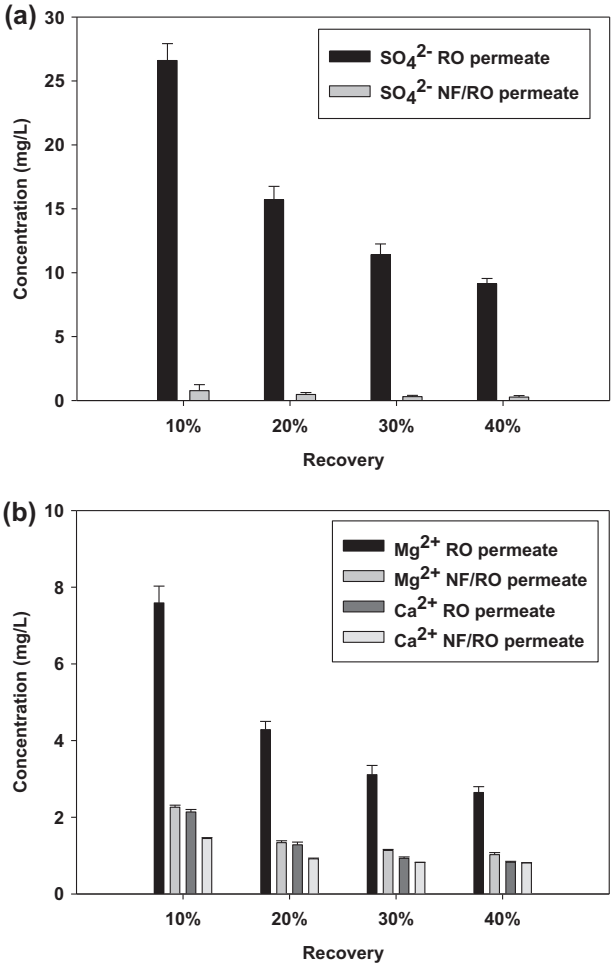

Fig. 5. Changes in concentrations of (a) sulfate and (b) magnesium and calcium ions, against RO recovery, with UF/RO permeate and UF/NF/RO permeate.

IonPac AS14 column (Dionex, USA) for anion analysis and DX-120 (Dionex, USA) equipped with IonPac CS12A column (Dionex, USA) for cation analysis. For anion analysis, 3.5 mM sodium carbonate and 1.0 mM sodium bicarbonate eluent (Dionex AS14 eluent concentrate, Thermo Scientific) were used, and 2.0 N sulfuric acid (Dionex, Sunnyvale, CA, USA) was used for anion regenerant. For cation analysis, methane sulfonic acid was purchased from Sigma-Aldrich and used for eluent. Tetrabutylammonium hydroxide solution (Fluka) was used as the cation regenerant solution. Silver-bonded resin cartridges (On-guard Ag, Dionex, Sunnyvale, USA) were used to remove chloride and sulfate anions prior to the IC analysis. Samples were diluted with different dilution factors to obtain reliable ion concentrations in the range 0.5–20 mg/L. Each permeate water quality from the experiments is listed in Table 4.

3. Results and discussions

As shown in Fig. 3, an NF membrane can effectively reject sulfate (SO_4^{2-}) and two cations (i.e. Mg^{2+}, Ca^{2+}) at high and moderate percentages, respectively, as expected from electrostatic repulsion interactions with the negatively charged membrane surface and the subsequent Donnan exclusion [18]. The NF membrane rejects Mg^{2+} more effectively than Ca^{2+}; however, molar concentrations of the two cations in the NF permeate were similar each other (Ca^{2+} concentration of 12.9 mM and Mg^{2+} concentration of 29.0 mM). Thus, it seems that any difference in rejection percentage between the two cations with NF membrane did not result from the different characteristics of the ions, such as size of the hydrated ions. As expected, the NF membrane did not reject all the monovalent ions, at virtually no rejection, from the UF permeate, as shown in Figs. 3(a) and 4(a). The two combinations of UF/RO and UF/NF/RO did not show any significant ion rejection performance (Fig. 3(b) and (c)).

Effects of recovery of the membrane systems were demonstrated in terms of sulfate rejection, with only the RO and NF/RO membranes. When the RO membrane was solely used (without NF membrane as pretreatment), sulfate levels in the permeates decreased with increasing recovery ratios, indicating that the process was dominated by diffusion over convection transport phenomena. However, the NF/RO combined system was not affected by variations in recovery ratios, probably due to fairly good sulfate rejection effectiveness of the NF membrane, as shown in Figs. 3(a) and 4(b). Rejection of divalent cations was also influenced by system recovery: even at relatively low recovery levels, Mg^{2+} levels decreased (i.e. increase in rejection) with increasing recovery, especially for the RO system, probably due to Donnan exclusion along with subsequent sulfate rejections. Calcium concentration in the permeate was less affected than magnesium; however, the Ca^{2+} levels still noticeably decreased, as shown in Fig. 5(b), for both RO and NF/RO systems.

Convection dominant process, with respect to ion rejection by NF membrane, was demonstrated by filtration experiments at temperatures in the range 5.0–28.5℃; decreased ion concentrations and TDS rejection were measured at relatively high seawater temperatures with increased permeate flux due to lower viscosity and corresponding lower membrane resistance (Fig. 6). In addition, this phenomenon can be explained by Arrhenius relation [17], This Arrhenius type of relation can elucidate the permeation behavior of either certain solutes or solvents through a membrane with increasing temperature, in terms of

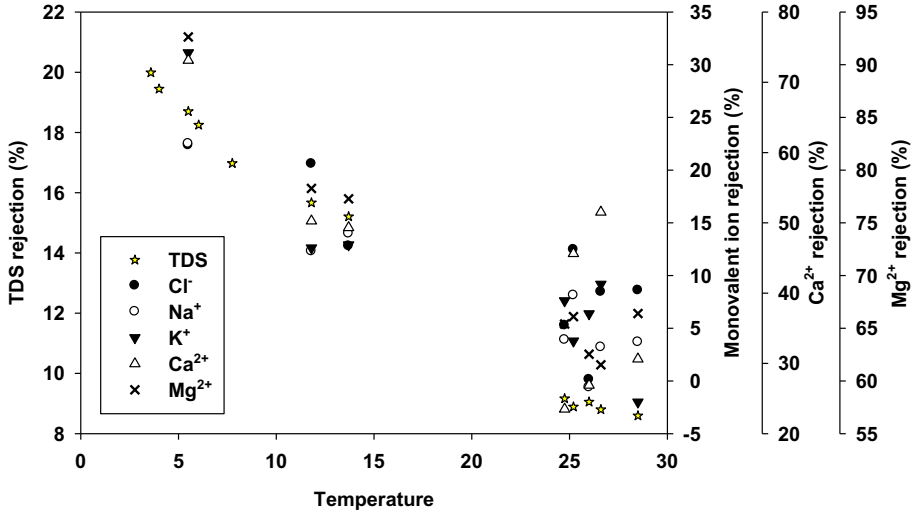

Fig. 6. Effect of temperature on the TDS, monovalent and divalent ions rejection (%) in NF system. % SO_4^{2-} rejection was not shown in this figure, but, sulfate rejection was from 96% at 28.5˚C to 99% at 5˚C.

activation energy and permeability coefficient. Otherwise, indirectly, this result can also be explained by membrane morphological changes, as discussed by Park et al. [19] and Sharma et al. [20]. According to Park et al., as temperature of feed water increased from 7 to 25˚C, molecular weight cutoff (MWCO) of the membranes also increased. Sharma et al. investigated the effect of temperature (5–41˚C) on two thin-film composite NF membranes and the results indicated that the morphology and structure of the polymer-based membrane barrier layer changed with increasing temperature. Membrane swelling has been also observed at different temperatures, as reported by Nilsson et al. At a higher temperature of 50˚C, the degree of swelling was more than that at 20˚C due to the increase in polymer flexibility at higher temperatures. Sulfate rejection was not affected by varying temperature and subsequent change in permeate flux, indicating that electrostatic repulsion was dominant over any other transport, for rejection of divalent sulfate anion.

Efficient operation of the NF/RO system was compared with the RO system, in terms of specific energy consumption (kWh/m^3) and TDS rejection, with different system recoveries. As shown in Fig. 7, the specific energy consumption of the NF/RO system decreased with increasing recovery ratio, similar to the RO system, with recovery ratios of 80% for the NF unit and 10–40% for the RO unit. The specific energy consumption of the NF/RO system ranged from 3.3 kWh/m^3 at 40% RO recovery to 9.9 kWh/m^3 at 10% RO recovery, with NF recovery ratio at 80%, for the relatively low-salinity seawater (TDS = 28,000 mg/L).

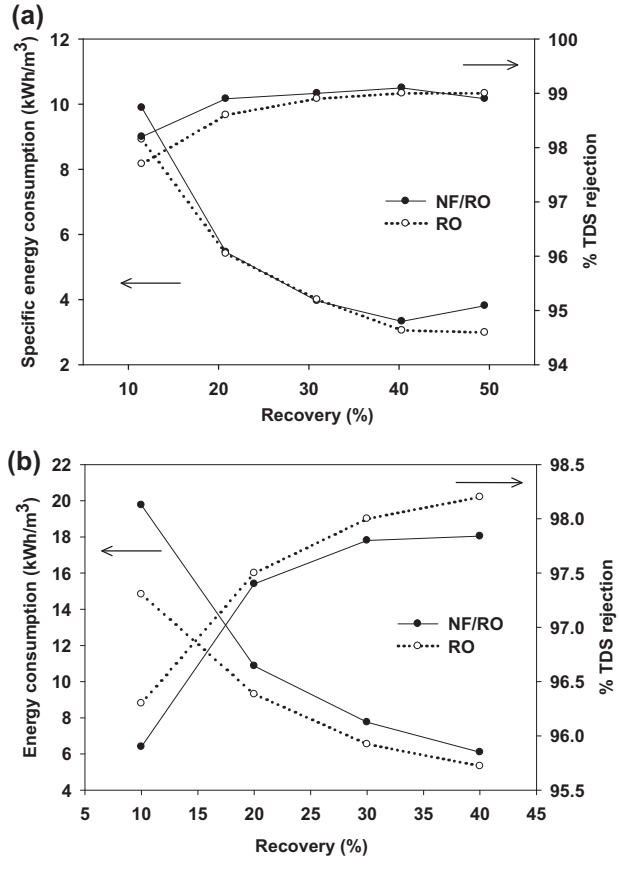

Fig. 7. Energy consumption and salt rejection of NF/RO hybrid system and only RO system for (a) seawater only and (b) designed seawater with different recoveries (NF recovery was set to 80% and RO recovery was 10–40%, Q_f = 40 m^3/d, All data are compensated at 25˚C).

In case of high-salinity seawater (TDS = 45,000 mg/L), the specific energy consumption of NF/RO (at NF recovery of 80%) ranged from 6.1 kWh/m^3 with 40% RO recovery to 19.8 kWh/m^3 with 10% RO recovery. The lowest levels of energy consumed by NF/SWRO (i.e. 3.3–6.1 kWh/m^3) are consistent with reported specific energy consumption values (3.7–5.3 kWh/m^3) [11–15]. However, when the recovery ratio decreased to 10–20%, the specific energy consumption significantly increased to 9.8–19.8 kWh/m^3.

Patterns of increasing TDS rejection of the NF/RO system were similar to the ones of the RO system. This demonstration with the NF/RO system was obvious at a relatively low TDS (~28,000 mg/L), generally found in the seas around Korea (Fig. 7(a)). However, when the salt levels of feed seawater increased to simulate a Middle East seawater TDS (~45,000 mg/L), the efficiencies in energy consumption and TDS rejection of the NF/RO system somewhat decreased compared to the RO system, but, the patterns were the same (Fig. 7(b)). The difference in energy consumption and TDS rejection was not significant; thus, it is probably compensated by somewhat increased water qualities, in terms of ion concentration levels in the final feedwater treated by the NF/RO system. Based on the specific energy consumption values for various types of seawaters containing low to high salt concentrations, the probable optimal operating condition for the NF/SWRO hybrid system can be the recovery ratio at 80% for NF and 40% for RO, which give the lowest specific energy consumption with relatively high salt rejections.

4. Conclusion

Combined system of NF/RO membranes was demonstrated for desalination, as compared to only-RO system, to identify some advantages in ion rejection performance (especially divalent ions) and system efficiencies. Even though no further scaling formation test or investigation into the foulant type were carried out, the system revealed increased water qualities of treated feed waters, in terms of divalent ions (including sulfate, magnesium, and calcium) especially at higher system recoveries at 80% for NF and 40% for RO. Effects of increased permeate flux with varying system recovery, and of water temperature on energy efficiency and ion rejection were demonstrated: either diffusion- or convection-dominant transport was identified using the ion rejections patterns of RO and NF membranes, respectively. The approaches adopted in this study can be further used to optimize both efficiency and effectiveness of the combined NF/RO system for better desalination, under varying operating conditions, even with different membranes.

Acknowledgments

This research was supported by the D-NARO (Daewoo-Nanofiltration Assisted Reverse Osmosis) Project grant funded by DAEWOO E&C, and also by the 2015 Research Fund (1.150049) of UNIST (Ulsan National Institute of Science and Technology).

The authors would like to acknowledge and thank Nari Lee, Keumju Yoon, Taewoo Nam, and Baekchon Tae for their valuable assistance in the water quality analysis. The first author acknowledges Gi-Ho Park, who supervised the project as a manager at DAEWOO E&C.

References

[1] K.P. Lee, T.C. Arnot, D. Mattia, A review of reverse osmosis membrane materials for desalination—Development to date and future potential, J. Membr. Sci. 370 (2011) 1–22.
[2] C. Fritzmann, J. Löwenberg, T. Wintgens, T. Melin, State-of-the-art of reverse osmosis desalination, Desalination 216 (2007) 1–76.
[3] IDA desalination yearbook 2011–2012, International Desalination Association (IDA), 2012.
[4] A.P. Mairal, A.R. Greenberg, W.B. Krantz, L.J. Bond, Real-time measurement of inorganic fouling of RO desalination membranes using ultrasonic time-domain reflectometry, J. Membr. Sci. 159 (1999) 185–196.
[5] M. Busch, W. Mickols, Reducing energy consumption in seawater desalination, Desalination 165 (2004) 299–312.
[6] C.A.C. van de Lisdonk, J.A.M. van Paassen, J.C. Schippers, Monitoring scaling in nanofiltration and reverse osmosis membrane systems, Desalination 132 (2000) 101–108.
[7] L. Llenas, G. Ribera, X. Martínez-Lladó, M. Rovira, J. de Pablo, Selection of nanofiltration membranes as pretreatment for scaling prevention in SWRO using real seawater, Desalin. Water. Treat. 51 (2012) 930–935.
[8] F. Dutoy, W. van der Wal, Successful antiscalant field trial—Optimization at higher pH and seawater temperature—Larnaca Desalination Plant, Desalin. Water Treat. 31 (2011) 311–319.
[9] P. Eriksson, M. Kyburz, W. Pergande, NF membrane characteristics and evaluation for sea water processing applications, Desalination 184 (2005) 281–294.
[10] A.A. Al-Hajouri, A.S. Al-Amoudi, A.M. Farooque, Long term experience in the operation of nanofiltration pretreatment unit for seawater desalination at SWCC SWRO plant, Desalin. Water. Treat. 51 (2012) 1861–1873.
[11] L. Llenas, X. Martínez-Lladó, A. Yaroshchuk, M. Rovira, J. de Pablo, Nanofiltration as pretreatment for scale prevention in seawater reverse osmosis desalination, Desalin. Water Treat. 36 (2011) 310–318.
[12] G.F. Leitner, Breaking the cost barrier for seawater desalting, Int. Desalin. Water Reuse Q 8 (1998) 15–20.
[13] S. Avlonitis, Operational water cost and productivity improvements for small-size RO desalination plants, Desalination 142 (2002) 295–304.

[14] M. Darwish, F. Al Asfourand N. Al-Najem, Energy consumption in equivalent work by different desalting methods: Case study for Kuwait, Desalination 152 (2003) 83–92.
[15] E. Drioli, A. Criscuoli, E. Curcio, Integrated membrane operations for seawater desalination, Desalination 147 (2002) 77–81.
[16] E. Drioli, E. Curcio, G. Di Profio, F. Macedonio, A. Criscuoli, Integrating membrane contactors technology and pressure-driven membrane operations for seawater desalination: Energy, exergy and costs analysis, Chem. Eng. Res. Des. 84 (2006) 209–220.
[17] M. Nilsson, G. Trägårdh, K. Östergren, The influence of pH, salt and temperature on nanofiltration performance, J. Membr. Sci. 312 (2008) 97–106.
[18] F.G. Donnan, Theory of membrane equilibria and membrane potentials in the presence of non-dialysing electrolytes. A contribution to physical-chemical physiology, J. Membr. Sci. 100 (1995) 45–55.
[19] N. Park, B. Kwon, M. Sun, H. Ahn, C. Kim, C. Kwoak, D. Lee, S. Chae, H. Hyung, J. Cho, Application of various membranes to remove NOM typically occurring in Korea with respect to DBP, Desalination 178 (2005) 161–169.
[20] R.R. Sharma, R. Agrawal, S. Chellam, Temperature effects on sieving characteristics of thin-film composite nanofiltration membranes: Pore size distributions and transport parameters, J. Membr. Sci. 223 (2003) 69–87.
[21] K. Plakas, A. Karabelas, T. Wintgens, T. Melin, A study of selected herbicides retention by nanofiltration membranes—The role of organic fouling, J. Membr. Sci. 284 (2006) 291–300.
[22] K.L. Tu, L.D. Nghiem, A.R. Chivas, Coupling effects of feed solution pH and ionic strength on the rejection of boron by NF/RO membranes, Chem. Eng. J. 168 (2011) 700–706.
[23] C.Y. Tang, Y.N. Kwon, J.O. Leckie, Fouling of reverse osmosis and nanofiltration membranes by humic acid —Effects of solution composition and hydrodynamic conditions, J. Membr. Sci. 290 (2007) 86–94.
[24] A. Widjaya, T. Hoang, G.W. Stevens, S.E. Kentish, A comparison of commercial reverse osmosis membrane characteristics and performance under alginate fouling conditions, Sep. Purif. Technol. 89 (2012) 270–281.